OPEN CHARM AND BEAUTY PRODUCTION

SANJAY PADHI

(ON BEHALF OF THE H1 AND ZEUS COLLABORATIONS)

Deutsches Elektronen-Synchrotron,
Notkestrasse 85, 22607 Hamburg, Germany
E-mail: spadhi@mail.desy.de

New results in open heavy flavour production in *ep* collisions are presented. Aspects sensitive to the various stages of the production mechanism are compared to the experimental data. Based on the measurements and the comparison with leading-order parton shower Monte Carlo models and next-to-leading order QCD predictions, conclusions related to data alone as well as model initiated issues are drawn.

1. Introduction

Open heavy quark production at HERA offers a novel way of testing both perturbative and non-perturbative aspects of quantum chromodynamics (QCD). For the quark to be "heavy", its mass[a] has to be larger than the QCD scale $\Lambda_{QCD} \sim 200$ - 300 MeV. Hence throughout this article, "heavy quark" will refer to a charm or a bottom quark. The following steps in heavy quark production can be distinguished (See Fig. 1 a):

- Hard subprocess: basic $2 \rightarrow 2$ process, e.g $\gamma g \rightarrow Q\bar{Q}$, boson gluon fusion (BGF) to form the heavy quark $Q\bar{Q}$ pair.
- Initial/Final state parton radiation.
- Fragmentation: transition of final state coloured partons to colourless hadrons.
- Unstable hadrons decay according to their branching ratios.

The first two stages are based on perturbative QCD (pQCD) calculations, while the last two rely on non-perturbative models. The cross section of a generic collision of two hadrons producing heavy quark pairs at HERA can

[a]The top quark, however, is too heavy and decays weakly before hadronizing.

be written as:

$$\sigma(S) = \sum_{i,j} \int dx_1 \int dx_2 f_i^{\gamma}(x_1, \mu_F) f_j^{p}(x_2, \mu_F) \hat{\sigma}_{ij}(x_1 x_2 S, m_Q^2, \mu_R^2) \quad (1)$$

where the cross section is a convolution of parton densities, $f_i^{\gamma}(x_1, \mu_F)$ and $f_j^{p}(x_2, \mu_F)$ of the photon and proton with the short distance cross section $\hat{\sigma}_{ij}$. The fractional hadronic momenta carried by the interacting partons are represented by x_1 and x_2 with μ_F and μ_R as the factorisation and renormalisation scales. The partonic cross section presented above further needs to be convoluted with a fragmentation function to obtain the hadronic cross section.

Two different collinear schemes and their combination are used for heavy quark production. In the massive-quark or fixed-order next-to-leading order scheme (FO NLO), the heavy quark Q is on-mass-shell and it only appears in the final state, but not as an active parton inside the incoming photon or proton. The calculation is expected to be valid for $p_T \sim m_Q$. However in the massless-quark scheme or zero-mass variable-flavour-number scheme (VFNS), the quark Q, (with $p_T > m_Q$) is treated as massless, such that it appears as an active parton of the incoming photon or proton, with a non perturbative parton density function. The attempt made to combine the results from FO NLO with suitably subtracted VFNS and with perturbative fragmentation functions (PFFs), resulted in the fixed order next-to-leading logarithm (FONLL) scheme[1]. The FONLL thus is expected to give more reliable predictions for heavy quark production.

1.1. *Experimental techniques*

The reconstruction of heavy quark mesons in the two HERA experiments H1 and ZEUS is based on either mass or lifetime tags. Due to the large b-quark mass H1 and ZEUS consider muons from semi-leptonic b-decays, which usually have high values of transverse momentum p_T^{rel}, with respect to the closest b quark initiated jet axis. The muons coming from charm and light quark decays have low values of p_T^{rel} as shown in Fig. 1(b). Also, the decay length of beauty is longer than that for charm and other light quarks. Hence the silicon vertex detector in H1 was used to tag the lifetime (see Fig. 1(c)) to distinguish beauty from other quarks.

The fraction of events from b-decays in a specific data sample[2] extracted on a statistical basis by adjusting the relative fractions of the simulated bottom, charm and light quarks decays to the measured p_T^{rel} and impact

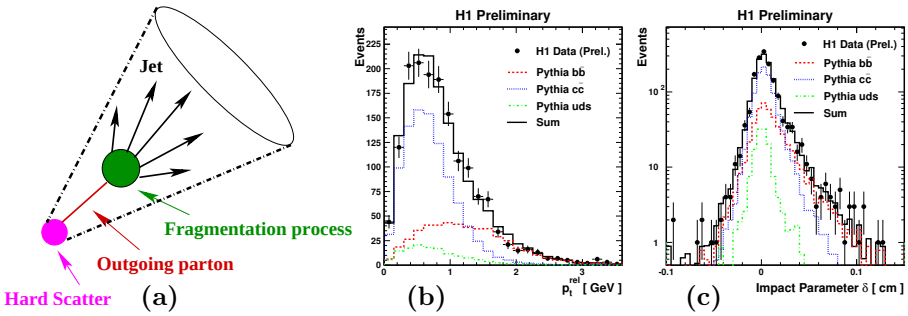

Figure 1. (a) Representation of the various stages of production and fragmentation of heavy quarks. The distribution of (b) the muon p_T^{rel} relative to the jet axis and (c) the impact parameter δ, of the muon track, are compared with the Monte Carlo simulations.

parameter δ distribution[b] is respectively found to be $f_b = 28.8 \pm 2.8\%$ and $f_b = 28.0 \pm 4.2\%$ in the H1 analysis. The two independent methods are found to be consistent in predicting the beauty fraction.

The charmed hadrons on the other hand are generally observed by forming the invariant mass of the tracks identified with a specific decay channel. In the presence of a vertex detector backgrounds can be reduced by measuring the displaced vertices from the primary interaction point. The recent measurement[3] by H1 for the charmed meson D^+, with a tag on the decay significance length, shows an improvement in signal to background ratio by a factor of $\sim \mathcal{O}(50)$.

In the following sections, results of open heavy quark production from HERA are discussed. Beauty, due to its large mass, is expected to have a faster convergence in the perturbative expansion in powers of the strong coupling constant α_s. Thus QCD calculations are expected to provide more reliable predictions for beauty than for charm, and will be discussed in the next section followed by the experimental results for open charm production.

2. Measurements of open beauty cross sections

One of the primary limitations of experimental measurements is the restriction of kinematic region, which is usually defined by the detector ac-

[b]The impact parameter δ is calculated in the plane transverse to the beam axis. Its magnitude is the distance of the closest approach of the track to the primary event vertex.

ceptance. Measurements performed in the restricted region are often extrapolated to the full phase space using a particular theoretical framework (either Monte Carlo models or next-to-leading order calculations), in order to compare between different experiments. As long as the model assumptions are not absorbed in the experimental results, but in the corresponding QCD predictions, the published measurements can be considered to be "safe".

On the other hand in the case of extrapolation to an unmeasured kinematic region, the extrapolation done should not only be quoted, but should also be compared within the same theoretical framework. For example the extrapolated cross section to an unmeasured phase space using a given Monte Carlo simulation cannot be reliably compared to the cross section predicted by a NLO calculation. Thus only those beauty measurements are considered here, where the measurements are made in the visible kinematic region without extrapolation.

The measurement of the beauty cross section by ZEUS[4] in the deep inelastic scattering (DIS) regime, using the p_T^{rel} method, as a function of Q^2 is shown in Fig. 2(a). The total visible cross section σ was determined in the kinematic range $Q^2 > 2$ GeV^2, inelasticity between $0.05 < y < 0.7$, with at least one jet in the Breit frame with $E_{T,jet}^{Breit} > 6$ GeV and pseudorapidity $\eta_{jet}^{Lab} < 2.5$, and with a muon between $30^\circ < \theta^\mu < 160^\circ$ and $p_T^\mu > 2$ GeV. The measured cross section is

$$\sigma = 38.7 \pm 7.7 \ \ (\text{stat.})^{+6.1}_{-5.0}(\text{syst.}) \ \ \text{pb.}$$

about a factor of 1.4 above the NLO QCD predictions of $28.1^{+5.3}_{-3.5}$ pb. It is, however, consistent with the measurement within the large theoretical and experimental uncertainties. The errors on the prediction were estimated by varying the factorisation and renormalisation scales by a factor of 2 and the b-quark mass between 4.5 and 5.0 GeV. CASCADE, based on the CCFM evolution equations, is in agreement with the measured cross section. The RAPGAP Monte carlo simulation based on DGLAP on the other hand lies below the data.

In order to obtain a unified picture on the beauty production H1[2] and ZEUS[5] recently measured the beauty cross section in the photoproduction regime within almost identical phase spaces. Fig. 2(b) shows the ratio of the measured cross section over theoretical expectations as a function of p_T^μ obtained either using the p_T^{rel} and δ method (H1) or the p_T^{rel} method (ZEUS). The low virtuality ($Q^2 < 1$ GeV^2), dijet photoproduction samples, are considered with $E_T^{jet1(2)} > 7(6)$ GeV, $|\eta^{jet}| < 2.5$ and

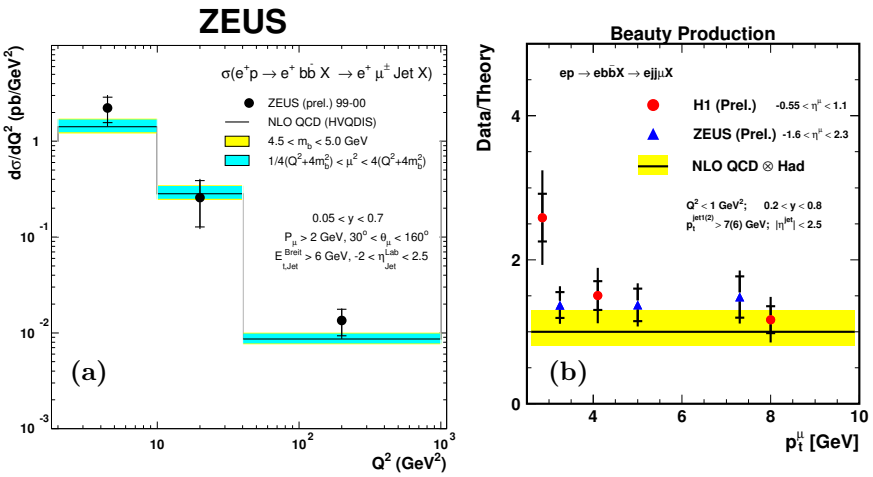

Figure 2. Beauty differential cross section (a) in DIS as a function of Q^2 with at least one reconstructed jet in the Breit frame in association with a muon and (b) the ratio of measured cross section over theoretical expectation, in the photoproduction regime as a function of p_T^μ, for events with two jets and a muon with $p_T^\mu > 2.5$.

$0.2 < y < 0.8$. The differential cross section as a function of the transverse momentum of the associated muons with $p_T^\mu > 2.5$ GeV and the pseudorapidity $-0.55 < \eta^\mu < 1.1$ (H1) or $-1.6 < \eta^\mu < 2.3$ (ZEUS) are found to be in agreement within the two experiments. The FO NLO QCD calculation is in reasonable agreement with the data within the large experimental and theoretical uncertainties, which are of similar size, except for the lowest p_T^μ H1 measured bin.

3. Measurements of open charm cross sections

Inclusive production of the charmed mesons D^+, D^0, D_s and D^+ in DIS was measured[3] with the H1 detector, using an integrated luminosity of 48 pb^{-1}. In these measurements the charm lifetime properties are exploited using a two layer silicon vertex detector. Differential cross sections are measured for the D^+ and D^0 mesons and compared with the AROMA MC predictions in the kinematic range $2 < Q^2 < 100$ GeV^2, $0.05 < y < 0.7$, $p_t(D) > 2.5$ GeV and $|\eta(D)| < 1.5$. Results for the D^+ channel are shown in Fig. 3(A). The distributions are well described both in shape and normalisation at LO with a parton shower QCD simulation. The lower shaded band indicates the AROMA beauty contribution, scaled by a factor of 4.3, according to

the H1 published values[6].

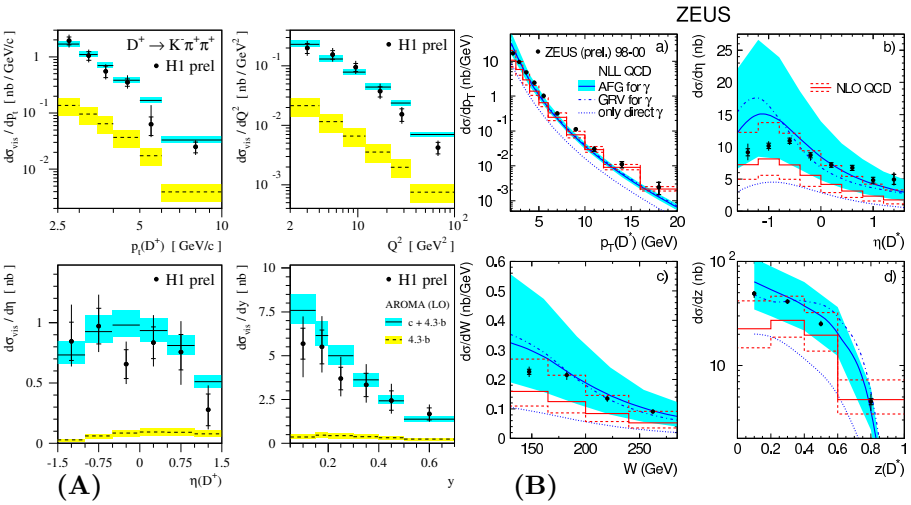

Figure 3. Differential cross section for (A) D^+ as a function of $p_t(D^+)$, Q^2, $\eta(D^+)$ and electron inelasticity y in the DIS regime, compared with the AROMA predictions and (B) inclusive D^* photoproduction events, as a function of a) $p_T(D^*)$, b) $\eta(D^*)$, c) $W(D^*)$ and d) $z(D^*)$. FO NLO predictions with nominal parameters are given by the solid histogram. The VFNS predictions (labeled as NLL) are shown by the solid curves. The GRV photon parameterisation and direct photon predictions are given by dash-dotted and dotted lines.

Inclusive photoproduction of D^* mesons has been measured[7] with the ZEUS detector in the kinematic region $Q^2 < 1$ GeV^2, γp centre-of-mass energies $130 < W < 280$ GeV, $1.9 < p_T(D^*) < 20$ GeV and $|\eta(D^*)| < 1.6$ using an integrated luminosity of 79 pb^{-1}. The measured differential cross sections were compared with FO NLO, VFNS and FONLL QCD predictions. In Fig. 3(B) the differential cross section as a function of a) $p_T(D*)$, b) $\eta(D^*)$, c) $W(D^*)$ and d) $z(D^*)$ are compared with the FO NLO and VFNS QCD calculations, where $z(D^*)$ is the fraction of the photon energy carried by the charmed meson in the proton rest frame. The precision of the data is enormously better than the theoretical uncertainties. The uncertainties for VFNS are larger than for the FO NLO calculations, which were obtained by varying the charm mass and the renormalisation scales simultaneously. The central FO NLO predictions are below the data, mainly in the proton direction ($\eta > 0$) and the low z region. The VFNS prediction is closer to the data, in particular it is better than FO NLO for $d\sigma/dz$ and

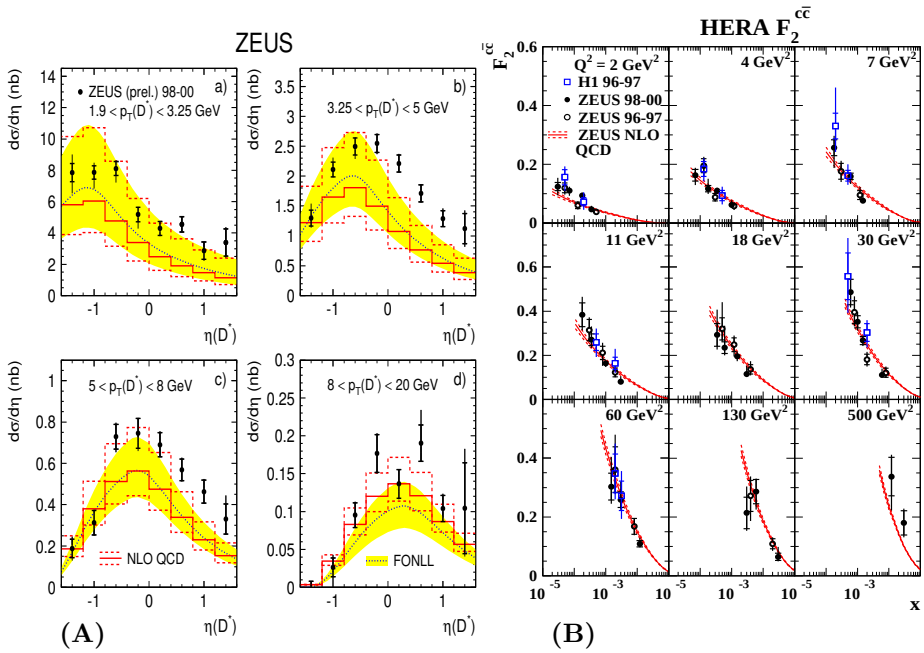

Figure 4. (A) Differential cross section $d\sigma/d\eta$ for inclusive D^* photoproduction in four p_T regions, compared to FO NLO (histograms) and FONLL (curves) predictions. (B) Charm contribution to the proton structure function for different Q^2 at a function of x.

for positive pseudorapidity. The direct photon processes alone in VFNS cannot describe the data distribution and hence a significant resolved contribution is required, which as expected shows sensitivity to the variation in the photon structure function parameterisations.

Given the precision of the ZEUS data, the differential cross sections for different $p_T(D^*)$ regions as a function of $\eta(D^*)$ are compared to the FO NLO and FONLL predictions in Fig. 4(A). This comparison allows to identify the region of phase space where the discrepancy between the data and the calculations can be localized. The data is close to the upper limit of the uncertainties of the predictions and is significantly above both the FO NLO and FONLL predictions at medium p_T and positive η. As expected due to the inherited properties from FO NLO, the FONLL is close to the former at low p_T, but is surprisingly below FO NLO at large p_T.

3.1. *Measurements sensitive to structure functions and hard scattering*

The photon acts as a pointlike probe of the proton in DIS, where the BGF (Fig. 5(e)) process dominates at HERA. This provides an unique opportunity to study the charm contribution $F_2^{c\bar{c}}$, to the proton structure F_2, which in turn is sensitive to the gluon density of the proton. The production of D^* mesons has been studied in DIS at HERA[8] in the kinematic region $1.5 < Q^2 < 1000$ GeV^2, $0.02 < y < 0.5$, $1.5 < p_T(D^*) < 15$ GeV and $|\eta(D^*)| < 1.5$. Predictions from NLO QCD are found to be in reasonable agreement with the measured differential cross section as a function of Q^2 and x. Hence this calculation was then used to extract $F_2^{c\bar{c}}$ using:

$$F_{2,\mathrm{meas}}^{c\bar{c}} = \frac{\sigma(x,Q^2)_{\mathrm{meas}}}{\sigma(x,Q^2)_{\mathrm{theo}}} \; F_{2,\mathrm{theo}}^{c\bar{c}}. \tag{2}$$

The extrapolation factors to the full phase space vary between 4.7 and 1.5 at low and high Q^2 respectively. The extracted $F_2^{c\bar{c}}$ are shown compared with the NLO QCD prediction in Fig. 4(B). A remarkable confirmation of the gluon density obtained from scaling violations of the inclusive F_2 can be observed within 10% accuracy. The data shows a steep rise at low x, indicating a large contribution of the gluon density in the proton. Since at low Q^2, the uncertainties of the data are comparable to those from the PDF fit, the measured differential cross section $\sigma(x, Q^2)$ should be used in future fits to constrain the gluon density of the proton.

In an analogous way, dijet photoproduction at HERA allows to study the structure of the photon. In leading order (LO) QCD the underlying sub-processes (Fig. 5) can be divided into either direct photon or resolved photon processes. In direct photon processes the photon participates in the hard scatter predominantly via the boson-gluon fusion process. Hence the fraction of the photon energy participating in the formation of two highest transverse energy jets, experimentally defined as x_γ^{obs}, is close to 1. On the other hand in resolved photon processes the photon acts like a source of incoming partons (quarks and gluons) and only a fraction of its momentum participates in the hard scatter, giving rise to $x_\gamma^{\mathrm{obs}} < 1$.

ZEUS recently measured such a photon energy fraction associated with at least one charm quark for dijet photoproduction events[9]. Fig. 6(a) shows the differential cross section as a function of x_γ^{obs} in comparison with PYTHIA, HERWIG and CASCADE. Not only a rise at high x_γ^{obs} is observed, there is a substantial tail at low x_γ^{obs}, which requires a significant ($\approx 40\%$) LO-resolved contribution to describe the data. The low x_γ^{obs}

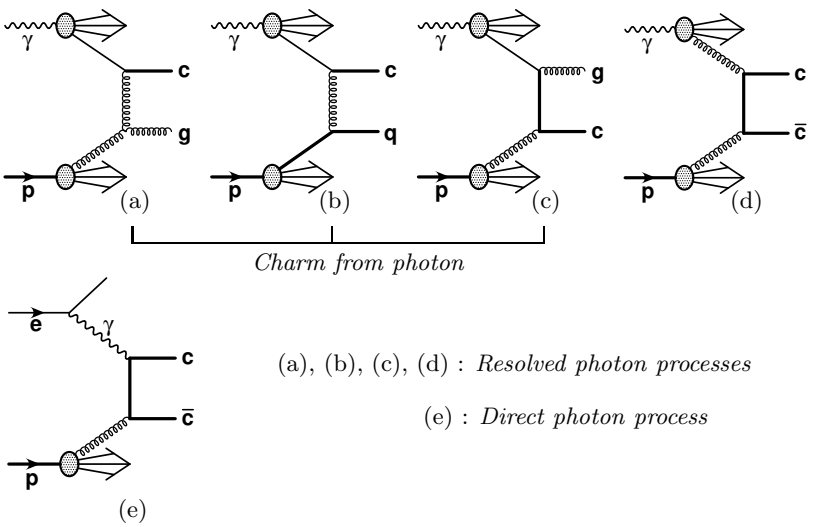

Figure 5. Various LO sub-processes with charm, dominant in the HERA region of phase space.

data are consistent with the presence of resolved photon processes, and can also be simulated in CASCADE via initial-state radiation based on CCFM evolution. However, CASCADE overestimates the high $x_\gamma^{\rm obs}$ region.

A similar study in both the γp and DIS regimes[10] with two high E_T^{jet} jets was done in order to probe the structure of the virtual photon. The ratio of the low and high $x_\gamma^{\rm obs}$ regions is shown in Fig. 6(b) and compared to CASCADE and AROMA expectations. The AROMA model using the DGLAP evolution scheme lies below the data, whereas CASCADE with CCFM evolution is much closer to the data. The fact that the ratio does not change significantly with Q^2 is in marked contrast to the case in which the presence of charm is not required[11], suggesting that the suppression of the low $x_\gamma^{\rm obs}$ cross section due to the charm mass and the suppression due to photon virtuality as the scales are not independent.

In order to probe the dynamics of the hard scattering in the sub-process (see Fig. 5) and in particular to study the charm content of the photon, the differential cross section $d\sigma/d|\cos\theta^*|$ as shown in Fig. 7(a), as a function of $|\cos\theta^*|$ was measured[9], where θ^* is the angle between the jet-jet axis and the beam direction in the dijet rest frame. The distribution was measured for resolved-enriched ($x_\gamma^{\rm obs} < 0.75$) and direct-enriched ($x_\gamma^{\rm obs} > 0.75$) samples. The cross section for the sample enriched with resolved photon events exhibits a more rapid rise towards high values of $|\cos\theta^*|$ than does

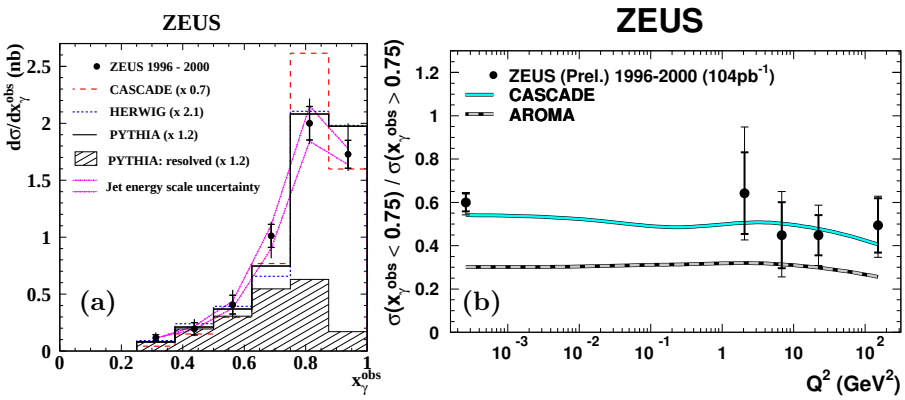

Figure 6. (a) Differential cross section $d\sigma/dx_\gamma^{\rm obs}$ for photoproduction events compared with MC simulations. Each MC distribution is normalised to the data, as indicated in the brackets. (b) Ratio of low to high x_γ^{obs} for events with a D^* compared to the predictions of AROMA and CASCADE, which do not include photon structure.

the cross section for the direct-enriched sample. The measured differential cross section in comparison to the LO partonic matrix elements reflects the different spins of the quark and gluon propagators in the dominant diagrams. Consequently the subprocess $gg \to c\bar{c}$ cannot be the dominant resolved photon process for the charm dijet events.

Independent of any model assumptions, the Rutherford scattering cross section for a q-exchange, $(\approx (1 - |\cos\theta^*|)^{-1})$ should show a mild rise, in contrast to the g-exchange diagram $\approx (1-|\cos\theta^*|)^{-2}$. To quantify this rise, the measured cross section for the direct and resolved enriched samples were fitted to a function $1/(1 - |\cos\theta^*|)^\kappa$. The resultant values of κ are:

$$\begin{aligned} \kappa(x_\gamma^{\rm obs} < 0.75) &= 1.735 \pm 0.176; \\ \kappa(x_\gamma^{\rm obs} > 0.75) &= 0.743 \pm 0.107 \end{aligned} \tag{3}$$

Given the fact that the shapes are expected to be distorted due to the additional parton radiation and hadronisation corrections, the results are consistent with the Rutherford scattering expectations.

The two jets are then distinguished into a charm-initiated jet (D^* jet), and the other jet in $\eta - \phi$ space (the variable $\Delta R_i \equiv \sqrt{(\phi_{jet_i} - \phi_{D^*})^2 + (\eta_{jet_i} - \eta_{D^*})^2}$) is used with the D^* jet having the smallest $\Delta R_{i(1=1,2)} < 1.0$. Thus the sign of the unfolded $\cos\theta^*$ distribution is given by the direction of the D^* meson. It is positive for the proton direction and negative for the photon direction.

Fig. 7(b) shows the differential cross section as a function of $\cos\theta^*$ for the

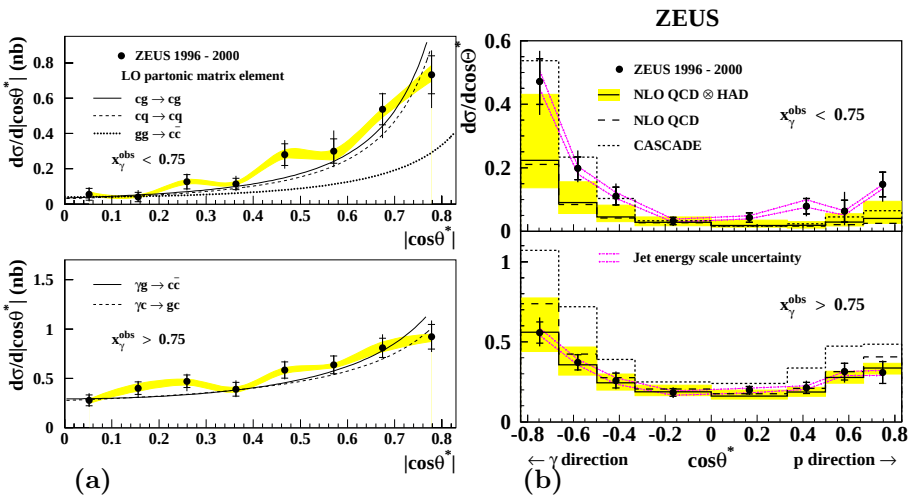

Figure 7. (a) Differential cross section $d\sigma/d|\cos\theta^*|$ for samples enriched in resolved and direct photon events, compared to leading order $2 \to 2$ matrix element with at least a charm in the final state. All matrix element distributions are normalised to the first data bin. (b) Differential cross section as a function of $\cos\theta^*$ for samples enriched in resolved and direct photon events compared with FO NLO predictions. The NLO uncertainty after hadronisation correction is given by the shaded band.

resolved- and direct-enriched samples. The $\cos\theta^*$ distribution for direct-enriched sample is almost symmetric, as expected from the BGF process. The slight asymmetry can be explained by the PYTHIA estimation[9] of the resolved process contribution to the direct enriched sample. The strong rise in the cross section towards the photon direction for the resolved-enriched sample is clear evidence for charm originating from the photon with a gluon propagator. Although the shape for low $x_\gamma^{\rm obs}$ events is reproduced by both CASCADE and the FO NLO predictions, the large uncertainties in the FO NLO prediction localized in the photon direction indicate non-convergent terms in the perturbative expansion due to collinear emissions of partons causing a large scale dependence. These terms then need to be absorbed either in the fragmentation or in the charm distribution functions of the photon and proton. Of course, to perform this absorption a charm contribution in the structure function is needed.

3.2. *Charm fragmentation*

The non-perturbative aspect of QCD was studied in terms of charm fragmentation. The data comparison to the theoretical predictions in all

hadronic colliders is done based on the assumption of universality in charm fragmentation. This assumption then allows to use the parameterisations of the fragmentation characteristics obtained in e^+e^- annihilations in the calculations for charm production in ep scattering. The measurements of these fragmentation characteristics at HERA will not only permit the verification of the universality of charm fragmentation, but also can significantly contribute to the understanding of the non-perturbative process.

The H1 and ZEUS measurements in the DIS[3] and photoproduction[12] regime respectively, were used to obtain preliminary results on the transfer of the quark's energy to a given meson. The fragmentation fractions of the charm quark to the various mesons are shown in Table 1. In addition H1 and ZEUS measured cross sections, which were used to test the isospin invariance of the fragmentation process by calculating the ratio of neutral $(c\bar{u})$ to charged $(c\bar{d})$ D meson production. The measured ratio $R_{u/d}$ is consistent with 1, confirming the isospin invariance. The s quark production is measured to be suppressed by a factor ≈ 3.5 as shown by γ_s. Both H1 and ZEUS rule out the naive spin counting prediction of 0.75 for the fraction of D mesons produced in a vector state P_V. The results in the table are compared with the e^+e^- world average values[13].

Table 1. The fractions of c quarks hadronising to a specific charmed meson. The results for $R_{u/d}$, γ_s and P_V are also provided, compared to the world average.

	H1 (DIS)	ZEUS (γp)	Combined e^+e^-
$f(c \to D^+)$	$0.20 \pm 0.02^{+0.04+0.03}_{-0.03-0.02}$	$0.249 \pm 0.014^{+0.004}_{-0.008}$	0.232 ± 0.010
$f(c \to D^0)$	$0.66 \pm 0.05^{+0.12+0.09}_{-0.14-0.05}$	$0.557 \pm 0.019^{+0.005}_{-0.013}$	0.549 ± 0.023
$f(c \to D_s^+)$	$0.16 \pm 0.04^{+0.04+0.05}_{-0.04-0.05}$	$0.107 \pm 0.009^{+0.005}_{-0.005}$	0.101 ± 0.009
$f(c \to \Lambda_c^+)$		$0.076 \pm 0.020^{+0.017}_{-0.001}$	0.076 ± 0.007
$f(c \to D^{*+})$	$0.26 \pm 0.02^{+0.06+0.03}_{-0.04-0.02}$	$0.223 \pm 0.009^{+0.003}_{-0.005}$	0.235 ± 0.007
$R_{u/d}$	$1.26 \pm 0.20^{+0.11+0.04}_{-0.11-0.04}$	$1.014 \pm 0.068^{+0.024}_{-0.031}$	1.00 ± 0.09
γ_s	$0.36 \pm 0.10^{+0.01+0.08}_{-0.01-0.08}$	$0.266 \pm 0.023^{+0.014}_{-0.012}$	0.26 ± 0.03
P_V	$0.69 \pm 0.045^{+0.004+0.009}_{-0.004-0.009}$	$0.554 \pm 0.019^{+0.008}_{-0.004}$	0.60 ± 0.03

The final uncertainty in the non-perturbative part of the QCD calculations is the fragmentation function, which affects both the shape and the absolute normalisation of the predicted cross section. It was recently measured by the ZEUS collaboration[14]. Charm associated jet events were used in the photoproduction regime in order to measure the jet energy fraction carried by a D^* meson defined as $z = (E + p_\parallel)_{D^*}/(E + p_\parallel)_{jet}$, where

the $p_{\|}$ is the longitudinal momentum of the D^* relative to the jet axis. The relative cross section shown in Fig. 8(a) is compared to the PYTHIA MC simulations with different values of the free parameter ϵ within the Peterson fragmentation function[15]. Strong sensitivity to the parameter ϵ, varied between 0.01 to 0.1 was found. The fit using χ^2 minimisation yields $\epsilon = 0.064 \pm 0.006^{+0.011}_{-0.008}$ in comparison to 0.053 from LO fits[16] to the LEP data. Although there are independent ways of measuring the fragmentation function, in Fig. 8(b) the OPAL and ARGUS results with different z definition are compared. They are similar in shape to the HERA data. The low-z peak in the OPAL data arises from a significant gluon-splitting due to the much higher centre-of-mass energy.

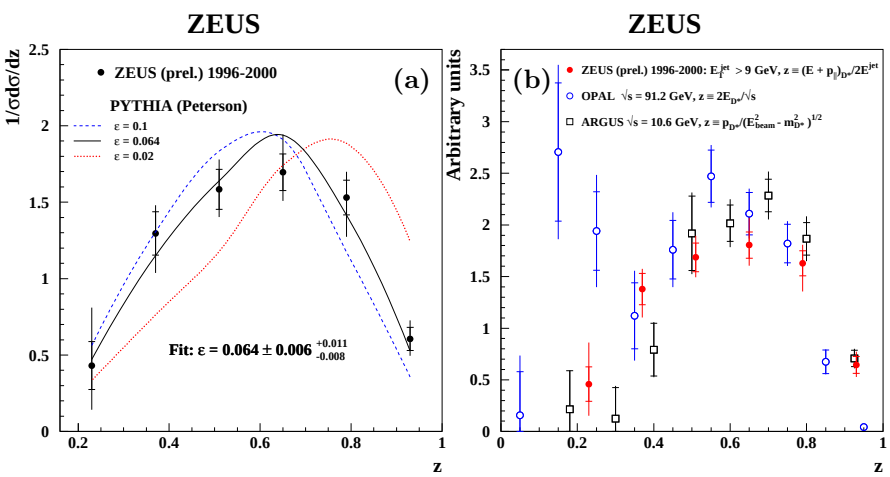

Figure 8. Relative cross section $1/\sigma d\sigma/dz$ for the data compared (a) with PYTHIA predictions for different values of the parameter ϵ in the Peterson fragmentation function and (b) to e^+e^- measurements, where the data sets are normalised to 1/(bin width) for $z > 0.3$.

The ZEUS fragmentation measurements are in good agreement with e^+e^- annihilations, indicating the universality of charm fragmentation.

4. Conclusions

Open heavy flavour measurements provide an important tool for understanding both perturbative and non-perturbative aspects of QCD. The QCD calculations do a fair job in describing the data, but fail within cer-

tain kinematic regions, and have large theoretical uncertainties. Beauty measurements made in almost identical kinematic phase spaces by the H1 and ZEUS experiments agree with each other. Very precise open charm measurements are made in both DIS and photoproduction.

Although the first HERA open charm signal consisted of 48 ± 11 events[17], with the enormous amount of available statistics, measurements sensitive to each aspect of the convolution ($\mathrm{PDF}_p \otimes \mathrm{PDF}_\gamma \otimes$ hard scatter $\otimes$ fragmentation) have been made. The recent trend at HERA not only includes the open beauty measurements in the visible range, but also structure function sensitive measurements like $F_2^{c\bar{c}}$, evidence of charm originating from the photon, multiscale issues with charm in deeply inelastic virtual photon scattering and of course new measurements of the charm fragmentation confirming the evidence of its universality.

References

1. M. Cacciari et al., *JHEP* **0103**, 6 (2001).
2. H1 Coll., Contributed paper to EPS 2003 conference, Abstract 117, Aachen, Germany, July 2003.
3. H1 Coll., Contributed paper to EPS 2003 conference, Abstract 096, Aachen, Germany, July 2003.
4. ZEUS Coll., Contributed paper to ICHEP02 conference, Abstract 783, Amsterdam, The Netherlands, July 2002.
5. ZEUS Coll., Contributed paper to ICHEP02 conference, Abstract 785, Amsterdam, The Netherlands, July 2002.
6. H1 Coll., S. Aid et al.*Phys. Lett.* **B 467**, 156 (1999).
7. ZEUS Coll., Contributed paper to ICHEP02 conference, Abstract 786, Amsterdam, The Netherlands, July 2002.
8. H1 Coll., Contributed paper to EPS2003 conference, Abstract 98, Aachen, Germany, July 2003; ZEUS Coll., S. Chekanov et al. DESY-03-115 (August 2003).
9. ZEUS Coll., *Phys. Lett.* **B 565**, 87 (2003).
10. ZEUS Coll., Contributed paper to EPS01 conference, Abstract 495, Budapest, Hungary, July 2001.
11. ZEUS Coll., Contributed paper to ICHEP00 conference, Abstract 1039, Osaka, Japan, July 2000.
12. ZEUS Coll., Contributed paper to EPS 2003 conference, Abstract 564, Aachen, Germany, July 2003.
13. L. Gladilin, Preprint hep-ex/9912064 (1999).
14. ZEUS Coll., Contributed paper to ICHEP02 conference, Abstract 778, Amsterdam, The Netherlands, July 2002.
15. C. Peterson et al., *Phys. Rev.* **D27**, 105 (1983).
16. P. Nason and C. Oleari, *Nucl. Phys.* **B 565**, 245 (2000).
17. ZEUS Coll., *Phys. Lett.* **B 349**, 225 (1995).